ELSEVIER

Journal of Alloys and Compounds 240 (1996) 139–150

Journal of ALLOYS AND COMPOUNDS

Magnetic ordering in ternary RMn_2Ge_2 compounds (R = Tb, Ho, Er, Tm, Lu) from neutron diffraction study

G. Venturini[a,*], B. Malaman[a], E. Ressouche[b]

[a]*Laboratoire de Chimie du Solide Minéral, Université Henri Poincaré-Nancy I, associé au CNRS (URA 158), B.P. 239, 54506 Vandoeuvre les Nancy Cedex, France*

[b]*CEA/Département de Recherche Fondamentale sur la Matière Condensée/SPSMS-MDN, 17 rue des Martyrs, 38054 Grenoble Cedex 9, France*

Received 6 February 1996

Abstract

The compounds RMn_2Ge_2 (R = Tb, Ho, Er, Tm, Lu) have been investigated by neutron diffraction. $TbMn_2Ge_2$ is a collinear ferrimagnet with the Mn and Tb moment aligned along the *c* axis ($\mu_{Tb} = 8.81(59)\ \mu_B$; $\mu_{Mn} = 2.21(44)\ \mu_B$). $HoMn_2Ge_2$ exhibits incommensurate ordering below 2.1 K characterized by two wavevectors at 1.3 K: $q_1 = (0.1543(4), 0.1543(4), 0)$ and $q_2 = (0.210(1), 0.007(1), 0)$. The Mn sublattice remains antiferromagnetic down to 1.3 K ($\mu_{Mn} = 2.38(6)\ \mu_B$). The Er moments order ferromagnetically below 5.5 K in $ErMn_2Ge_2$ ($\mu_{Er} = 6.81(31)\ \mu_B$). The moments are perpendicular to the *c* axis. The Mn sublattice remains antiferromagnetic down to 1.8 K ($\mu_{Mn} = 2.34(18)\ \mu_B$). The magnetic structure of $TmMn_2Ge_2$ is characterized by the propagation vector (0,0,1/2), the Tm moments lying in the basal plane. The ordering of the Tm moments yields a canting of the Mn moments ($\theta = 21(3)°$); $\mu_{Tm} = 6.63(18)\ \mu_B$; $\mu_{Mn} = 2.28(27)\ \mu_B$). The antiferromagnetic structure of $LuMn_2Ge_2$ has been determined ($\mu_{Mn} = 2.32(14)\ \mu_B$). The evolution of the magnetic properties of the heavy rare earth compounds RMn_2Ge_2 is discussed.

Keywords: Rare earth manganese germanides; Neutron diffraction; Magnetic structure determination; Magnetic properties

1. Introduction

Previous neutron diffraction studies on ternary RMn_2Ge_2 compounds (R = La–Nd) [1,2] have shown that a large component of the Mn moments is quenched into an antiferromagnetic arrangement within the (001) Mn planes. This is in contrast with the studies on yttrium and heavier rare earth compounds (Tb–Er) where the Mn planes are purely ferromagnetic [3–6]. Moreover, in the lightest rare earth compounds, the Mn moments are significantly larger than those measured in compounds characterized by ferromagnetic planes.

In order to complete this investigation, it was first planned to check the order and the magnitude of the Mn moment in the heaviest rare earth compounds, $TmMn_2Ge_2$ and $LuMn_2Ge_2$.

However, during this study, Purwanto et al. [7] pointed out the strong discrepancies concerning the magnetic structure of $TbMn_2Ge_2$ previously reported by Leciejewicz and Szytula [8]. Simultaneously, Gil et al. [9] reported on the magnetic order of a number of $CeNiSi_2$-type compounds RMn_xGe_2 (R = Nd, Tb, Ho). The analysis of these three works suggests that the low temperature behaviour of $TbMn_2Ge_2$ proposed by Leciejewicz and Szytula [8] has to be related to the magnetic ordering of non-negligible amounts of an impurity phase, $TbMn_{0.5}Ge_2$.

A similar conclusion could be stated concerning the magnetic behaviour of the Ho sublattice in $HoMn_2Ge_2$. According to Shigeoka [10], the holmium moments remain disordered at 4.2 K whereas, according to Leciejewicz et al. [11], neutron diffraction analysis yields an incommensurate magnetic structure at 7 K. Analysis of the corresponding neutron diffraction data points out a number of discrepancies particularly related to the observed and calculated Bragg angles. Moreover, the positions of the magnetic peaks are close to those measured in the $CeNiSi_2$-type RMn_xGe_2 compounds [9]. These observations would

* Corresponding author.

PII S0925-8388(96)02272-4

thus suggest that small amounts of $HoMn_xGe_2$ may also have contaminated this sample.

Bearing in mind the above mentioned uncertainties, it was finally decided to reinvestigate the whole RMn_2Ge_2 series (R = Tb–Tm, Lu) by neutron diffraction.

2. Experimental procedures

The samples were prepared from commercially available high purity elements. Pellets of stoichiometric amounts were melted in an induction furnace with the cold crucible apparatus. The resulting ingots were annealed for 2 weeks at 1173 K. Purity of samples was determined with the use of a powder X-ray diffraction technique (Guinier Cu Kα).

The magnetic measurements were carried out on a Faraday balance (between 300 and 700 K) and on a MANICS magneto-susceptometer (between 4.2 and 300 K) in fields up to 1.5 T.

Neutron experiments were carried out at the CEN Grenoble. The diffraction patterns were recorded with a one-dimensional curved multidetector DN5 with wavelength $\lambda = 2.489$ Å. In order to correct texture effects, a fitted coefficient (r_c) which reflected the importance of the preferential orientation was used during refinement.

Using the scattering lengths $b_{Ge} = 0.8185$, $b_{Mn} = -0.373$, $b_{Tb} = 0.738$, $b_{Ho} = 0.801$, $b_{Er} = 0.779$, $b_{Tm} = 0.707$ and $b_{Lu} = 0.721$ fm and the form factor of Mn and R^{3+} from Refs. [12,13], the refinements of the scaling factor, the z_{Ge} atomic position, r_c and the magnetic moments were carried out by the MiXeD crystallographic executive for diffraction (MXD) using a least squares fitting procedure [14].

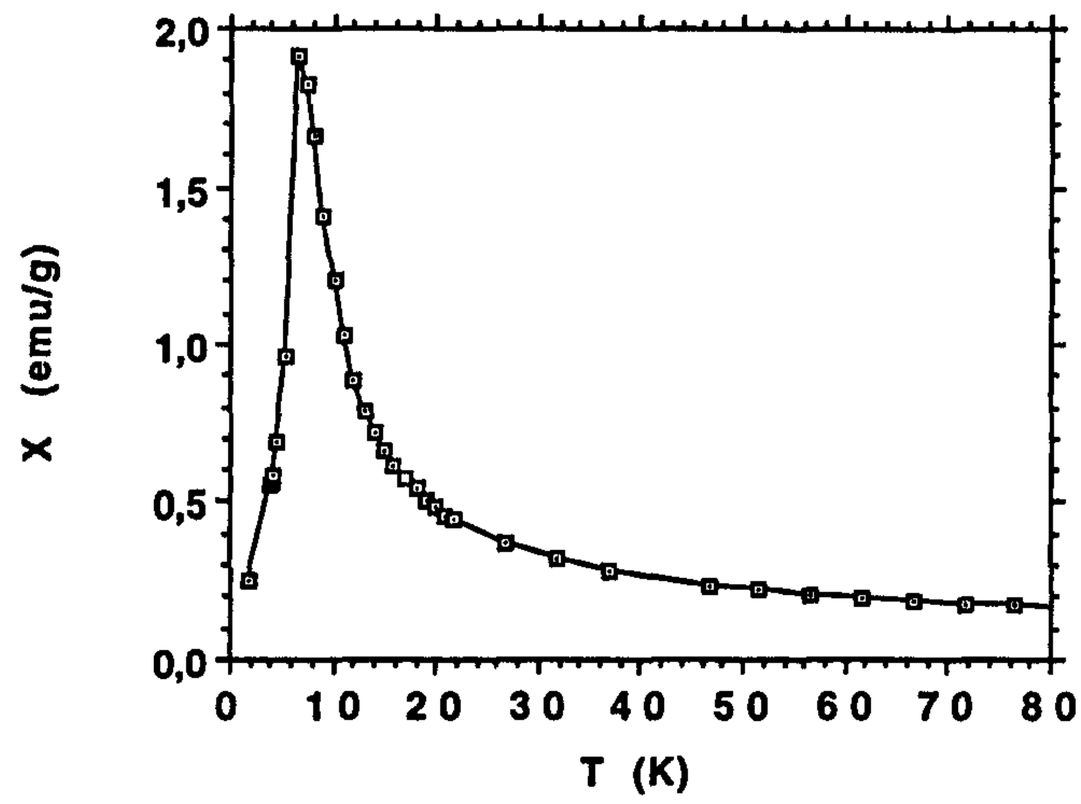

Fig. 1. $TmMn_2Ge_2$: thermal variation of the susceptibility at low temperature ($H_{appl} = 0.2$ T).

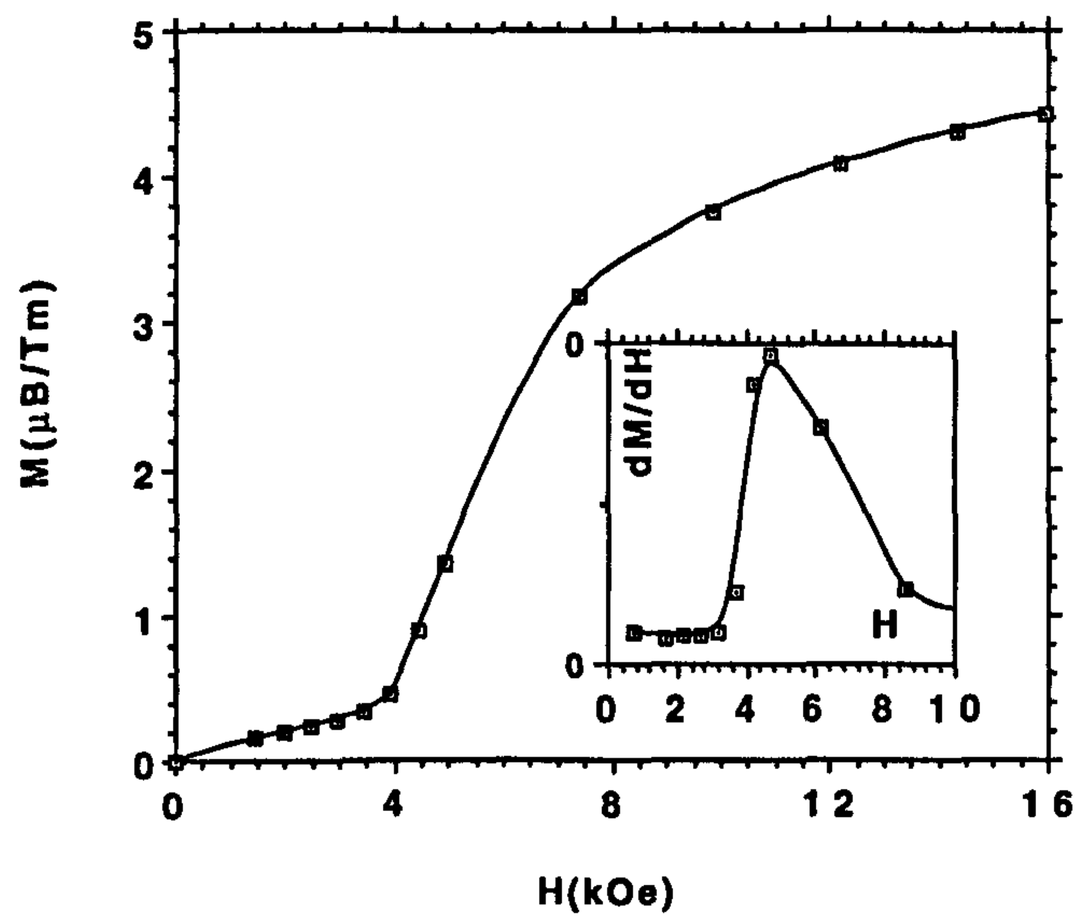

Fig. 2. $TmMn_2Ge_2$: magnetization curve at 4.2 K.

3. Results

3.1. Magnetic measurements

A detailed study on RMn_2Ge_2 (R = Gd–Er) single crystals has been previously undertaken by Shigeoka [10]. All these compounds are antiferromagnetic above room temperature while the R sublattice (R = Gd–Dy, Er) orders at low temperature. Moreover, it was previously shown that $LuMn_2Ge_2$ behaves antiferromagnetically below $T_N = 508$ K [15]. Therefore, in the present work we limited our investigations on the magnetic behaviour of the $TmMn_2Ge_2$ compound. In agreement with the whole RMn_2Ge_2 series, the Mn sublattice orders antiferromagnetically below $T_N = 487(\pm 5)$ K. The thermal variation of susceptibility and the field dependence of magnetization recorded at low temperature are displayed in Figs. 1 and 2. A sharp maximum, related to the Tm sublattice ordering, is observed at $T_N = 7.0 \pm 0.5$ K. At 4.2 K, $TmMn_2Ge_2$ exhibits a metamagnetic behaviour with a rather low threshold field value ($H_s \approx 0.5$ T).

3.2. Neutron diffraction study

3.2.1. $TbMn_2Ge_2$

The neutron diffraction patterns recorded at 130 and 2 K are presented in Fig. 3, thus confirming unambiguously the magnetic behaviour reported by Purwanto et al. [7]. At 2 K, the magnetic structure consists of antiferromagnetic coupling of both ferromagnetic Mn and Tb sublattices, the moments being aligned along the c axis (Fig. 4). The observed and calculated intensities and the refined parameters are gathered in Table 1. The moment of terbium ($\mu_{Tb} =$

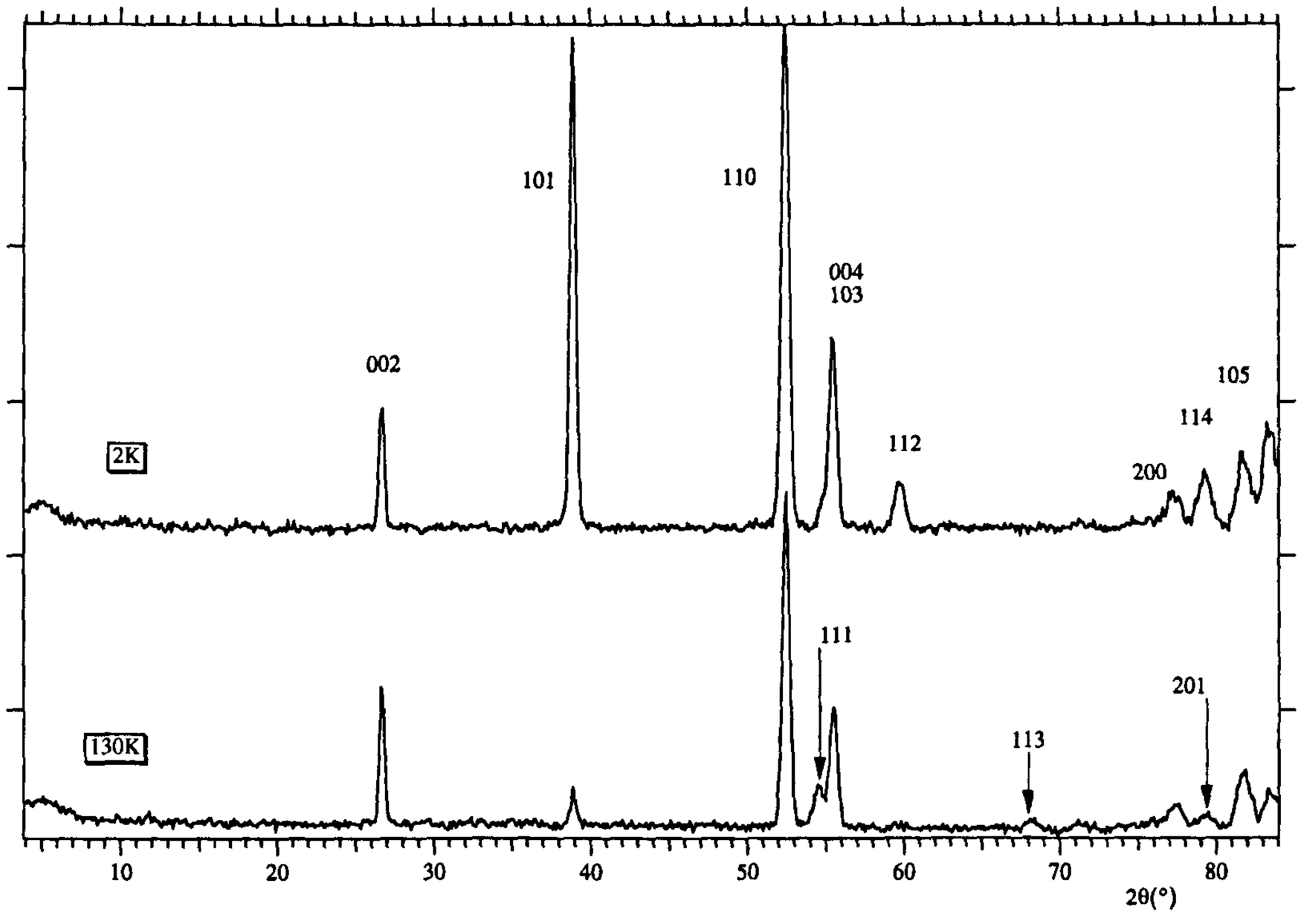

Fig. 3. $TbMn_2Ge_2$: neutron diffraction patterns at 2 and 130 K.

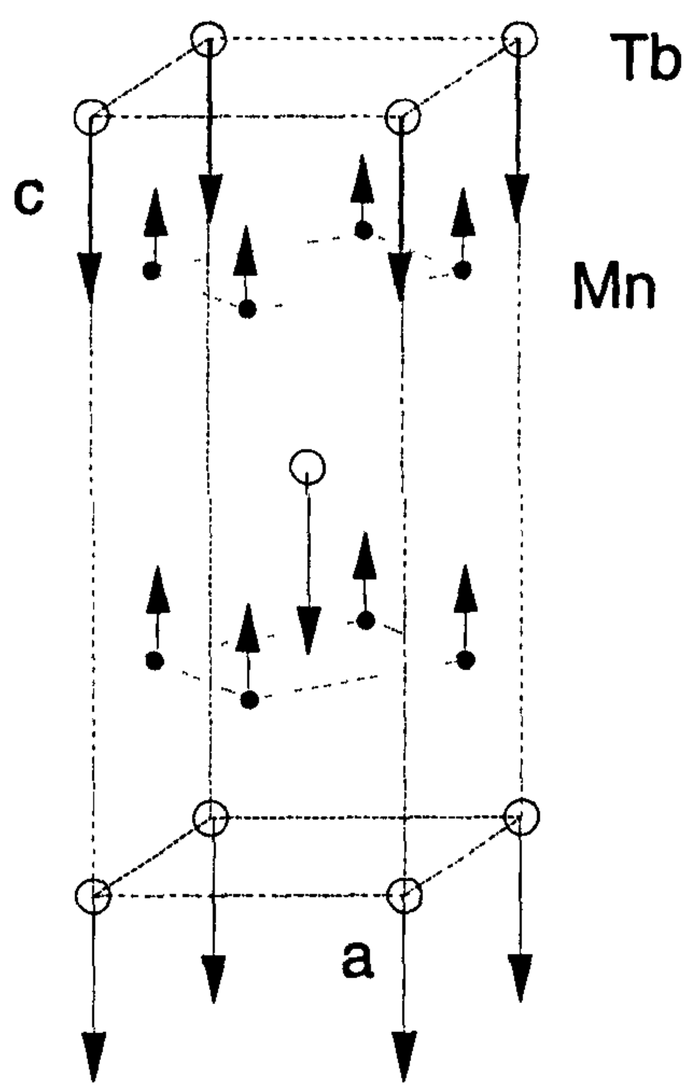

Fig. 4. Magnetic structure of $TbMn_2Ge_2$ at 4.2 K.

8.81 μ_B) is close to the free ion value ($gJ = 9\ \mu_B$), while the Mn moment ($\mu_{Mn} = 2.21\ \mu_B$) is close to those previously measured in the YMn_2Ge_2, $DyMn_2Ge_2$ and $ErMn_2Ge_2$ compounds [3–6]. The total magnetization at 2 K, calculated from the above values ($M \approx 4.4\ \mu_B$) is close to that measured by Shigeoka ($M \approx 5.3\ \mu_B$) [10]. The Curie temperature estimated from the thermal variation of the (101) line intensity is $T_c = 105 \pm 5$ K (Fig. 5). The thermal variation of the cell parameters indicates a positive striction of the parameter a at T_c while parameter c remains almost unchanged (Fig. 6). Both variations lead to a positive thermal expansion $\Delta l/l \approx 9 \times 10^{-4}$, at the Curie point, in good accord with the value measured by Shigeoka [10]. The thermal dependences of a and c do not exhibit inverted variations at T_c as previously observed in $SmMn_2Ge_2$ when spontaneous magnetization appears at low temperature [16,17].

3.2.2. $HoMn_2Ge_2$

Neutron diffraction patterns at various temperature are presented in Fig. 7. The sample was found to be contaminated by a small amount of $HoMn_{0.5}Ge_2$ as affirmed by the presence of the (131) line at $2\theta \approx 60°$.

Below 7 K, additional magnetic lines appear, mainly in the 2θ range 15–25°. The corresponding d spacings are obviously those observed by Leciejewicz et al. and which were unfortunately attributed to the $HoMn_2Ge_2$ magnetic ordering [11]. At 4 K, with the propagating vector (1/2,1/2,0), these magnetic lines are properly indexed in the $HoMn_{0.5}Ge_2$ cell.

Below $T_N = 2.5 \pm 0.1$ K, the ordering of the holmium moments in $HoMn_2Ge_2$ is observed. At 2.1 K, the observed lines are well indexed considering the propagating vector $q_1 = (q_x, q_y, 0)$ where $q_x = 0.142(2)$ and $q_y = 0.169(2)$. The thermal variation of the corresponding Bragg angles indicates that the components

Table 1
Observed and calculated intensities and corresponding refined parameters for $TbMn_2Ge_2$ at 133 at 2 K

	133 K		2 K	
h k l	F_c^2	F_o^2	F_c^2	F_o^2
0 0 2	18.3	18.6(4)	18.8	18.1(4)
1 0 1	9.6	9.6(7)	160.2	153(1)
1 1 0	208.4	209(2)	343.5	349(3)
1 1 1				
0 0 4	44.7	40(2)	18.0	14(2)
1 0 3	86.6	87(2)	150.2	146(2)
1 1 2	1.5	2(1)	37.3	51(2)
1 1 3	7.6	9(2)	0	0
2 0 0	50.2	56(4)	71.5	73(2)
2 0 1				
1 1 4	11.4	27(3)	87.6	113(3)
1 0 5	134.9	132(3)	153.2	155(3)
a(Å)	4.985(2)		3.986(2)	
c(Å)	10.818(5]		10.821(5)	
r_c	1.12(1)		1.07(3)	
z_{Ge}	0.385(1)		0.383(4)	
$\mu_{Mn}(\mu_B)$	1.77(20)		2.21(44)	
$\mu_{Tb}(\mu_B)$	0		8.81(59)	
R(%)	6.1		6.6	

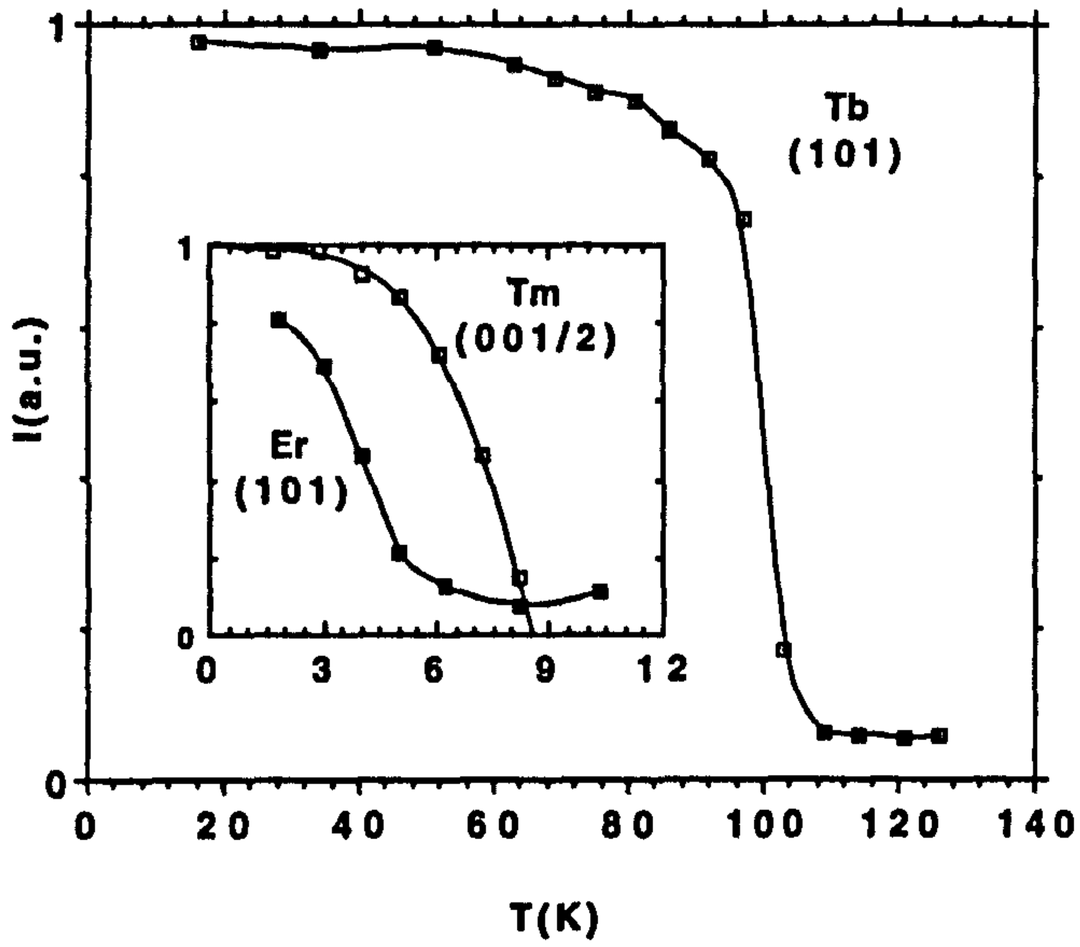

Fig. 5. Thermal variation of the intensities of some characteristic magnetic peaks of RMn_2Ge_2 compounds (R = Tb, Er, Tm).

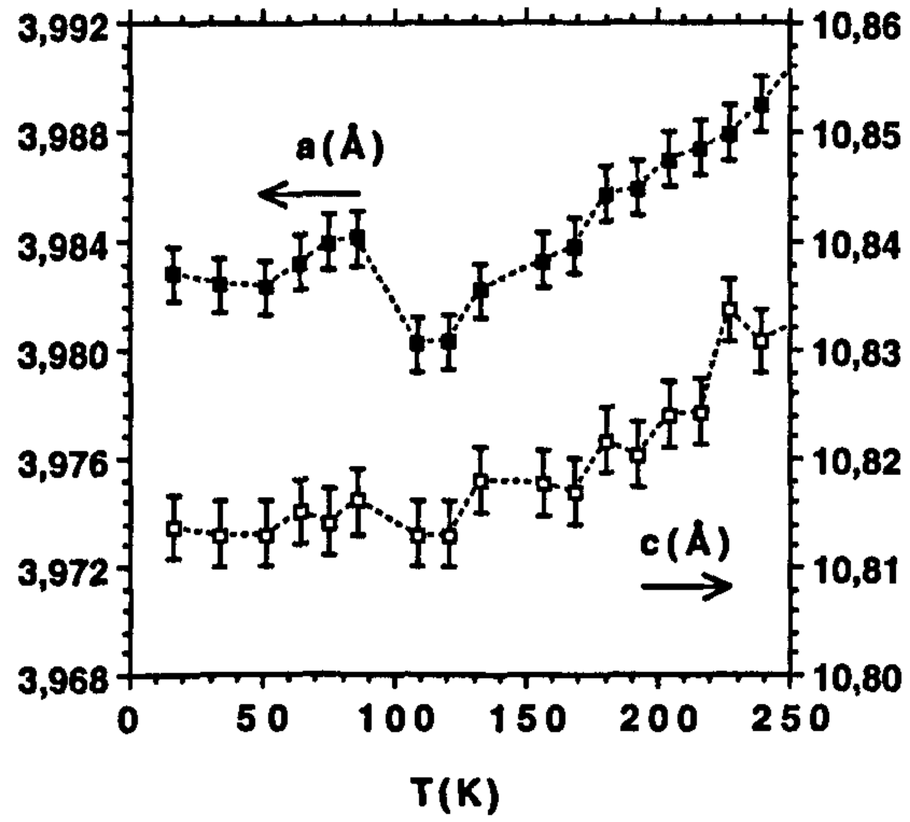

Fig. 6. Thermal variation of $TbMn_2Ge_2$ cell parameters.

of the propagating vector vary with temperature (Fig. 8). At 1.3 K, the refined values $q_x = q_y = 0.1543(4)$ suggest a wavevector of type $(q_x,q_x,0)$, in good accordance with the fine linewidth of the involved satellites.

Below $T_t = 2.1 \pm 0.2$ K, apart from the previously observed lines, a new system of lines appears. These peaks can also be indexed in the $HoMn_2Ge_2$ cell, considering the propagating vector $q_2 = (q_x', q_y', 0)$ where $q_x' = 0.210(1)$ and $q_y' = 0.007(1)$. The weak value of q_y' accounts for the width of the (hkl) satellites where $k \neq 0$.

The thermal variation of the intensity of two characteristic lines corresponding to q_1 and q_2 wavevectors is given in Fig. 9.

The refinement at 1.3 K was undertaken considering an inhomogeneous mixtures of two different magnetic structures for the holmium sublattice. Results are gathered in Table 2. Both magnetic structures may be described as sine-modulated structures. The direction of the Ho moment is, within the standard errors, aligned along the c axis in good accord with single crystal magnetization measurements [10]. The high temperature antiferromagnetic ordering of the Mn moments persists down to 1.3 K. Both holmium magnetic arrangements are illustrated in Fig. 10. The

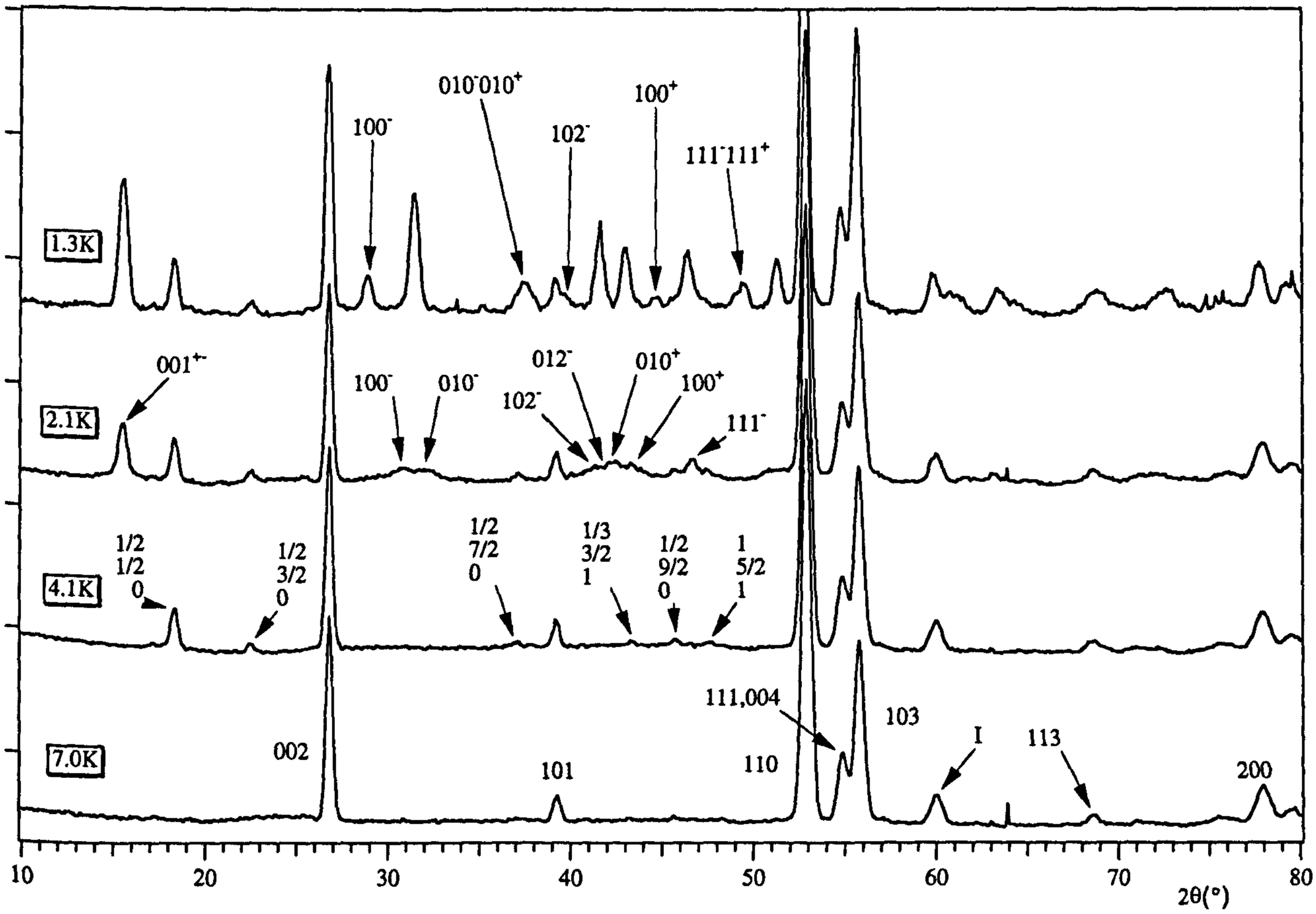

Fig. 7. $HoMn_2Ge_2$: neutron diffraction patterns at various characteristic temperatures. The Miller indices at 4.1, 2.1 and 1.3 K correspond to magnetic impurity lines, wavevector q_1 and wavevector q_2 respectively.

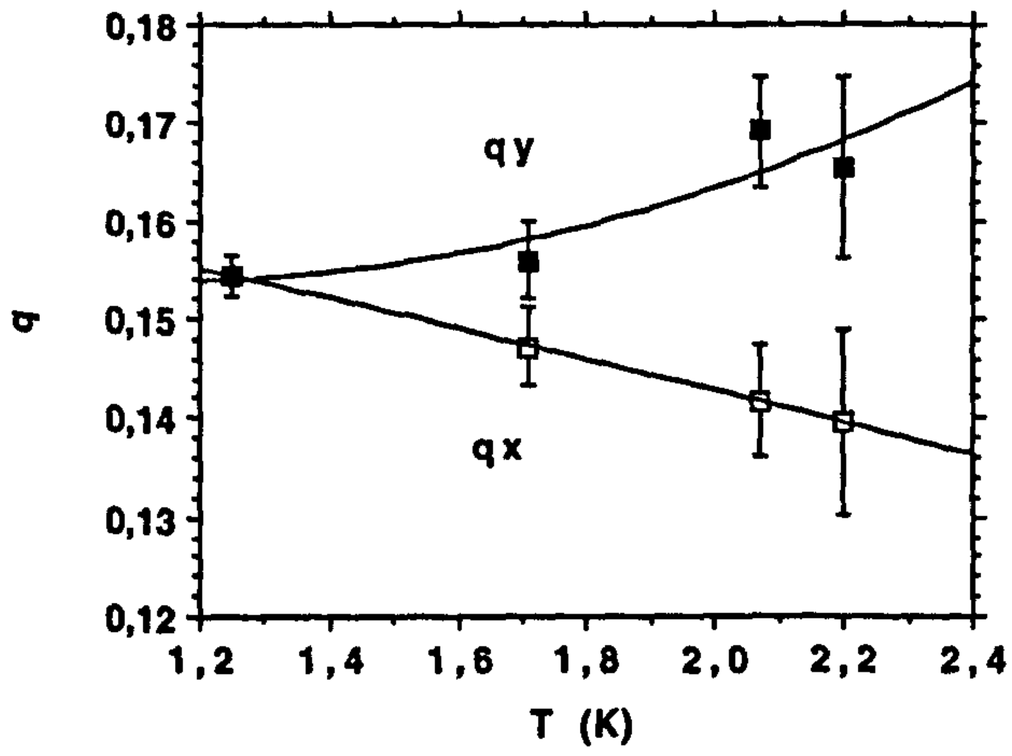

Fig. 8. $HoMn_2Ge_2$: thermal variation of the components of wavevector q_1.

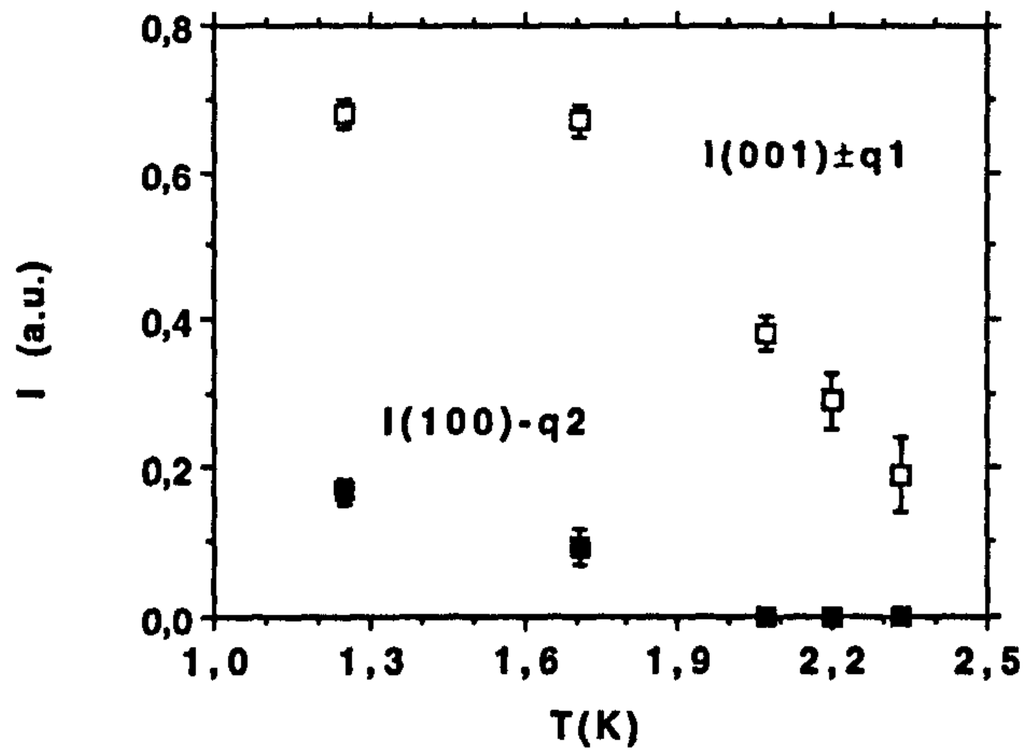

Fig. 9. $HoMn_2Ge_2$: thermal variation of the intensity of characteristic peaks related to wavevectors q_1 and q_2.

actual behaviour may, in fact, be a combination of both arrangements leading to a complicated magnetic structure, as previously observed in the case of $ErPd_2Si_2$ and $DyAg_2Si_2$ [18,19] where two propagating vectors are also observed.

3.2.3. $ErMn_2Ge_2$

Neutron diffraction patterns recorded at 12 and 1.8 K are presented in Fig. 11. They confirm the results obtained by Leciejewicz et al. [6]. The corresponding observed and calculated lines and refined parameters

Table 2
Observed and calculated Bragg angles and structure factors for $HoMn_2Ge_2$ at 1.3 K

$h\,k\,l$	θ_c	θ_o	F_c^2	F_o^2
$0\,0\,1 \pm q_2$	15.205			
$0\,0\,1 \pm q_1$	15.358	15.307	39.1	37.9(4)
$0\,0\,2$	26.547	26.559	152.5	162(1)
$1\,0\,0 - q_2$	28.679	28.686	26.2	33(1)
$1\,0\,0 - q_1$	31.257	31.246	125.6	134(1)
$0\,1\,0 - q_2$	37.089	37.076		
$0\,1\,0 + q_2$	37.609	37.597	49.9	64(2)
$1\,0\,1$	38.992	39.023	45.0	49(2)
$1\,0\,2 - q_2$	39.476	39.660	23.0	20(2)
$0\,0\,1 \pm q_2$	41.050			
$0\,0\,3 \pm q_1$	41.112			
$1\,0\,2 - q_1$	41.460	41.421	136.0	152(2)
$1\,0\,0 + q_1$	42.808	42.816	116.8	131(2)
$1\,0\,0 + q_2$	44.555	44.474	23.7	31(2)
$1\,1\,1 - q_1$	46.156			
$0\,1\,2 - q_2$	46.190			
$0\,1\,2 + q_2$	46.625	46.224	161.5	141(2)
$1\,1\,1 - q_2$	48.905	48.822		
$1\,1\,1 + q_2$	49.322	49.327	82.7	85(2)
$0\,1\,0 + q$	51.083	51.092	116.8	119(2)
$1\,1\,0$	52.614	52.603	1371.9	1369(5)
$1\,1\,1$	54.491			
$0\,0\,4$	54.671			
$1\,-1\,0 + q_1$	55.147	55.990	381.6	392(4)
$1\,0\,3$	55.502	55.491	708.9	710(4)
$1\,-1\,1 + q_2$	60.491	60.570		
$1\,1\,1 + q_2$	60.852			
$1\,1\,3 - q_1$	61.197	61.215	131.1	135(4)
$1\,0\,4 - q_2$	62.897			
$1\,1\,1 + q_1$	63.240	63.232		
$1\,1\,3 - q_2$	63.484			
$1\,-1\,3 - q_2$	63.836			
$1\,0\,4 - q_1$	64.334	64.178	175.3	171(3)
$1\,1\,4 - q_2$	67.916			
$0\,1\,4 + q_2$	68.255			
$1\,1\,3$	68.286	68.322		
$1\,-1\,3 + q_1$	68.832	68.928	223.8	200(5)
$2\,0\,1 - q_2$	69.872	70.030	36.1	45(5)
a(Å)	3.968(2)			
c(Å)	10.832(8)			
r_e	1.06(1)			
z_{Ge}	0.3836(11)			
$\mu_{Ho1}(\mu_B)$	7.43(17)			
$\mu_{Ho2}(\mu_B)$	4.76(21)			
$\mu_{Mn}(\mu_B)$	2.38(6)			
R(%)	2.8			

are gathered in Table 3. The erbium moments lie in the (001) planes in fair agreement with Shigeoka's results [10]. There is no significant indication of a possible canting of the Mn moments at the transition temperature, thus indicating that the ordering of the Mn moments remains unchanged in its high temperature antiferromagnetic arrangement. The thermal variation of the (101) line intensity leads to the Curie temperature $T_c = 5.5 \pm 0.5$ K (Fig. 5) in fair agreement with heat capacity studies ($T_c = 5.1$ K) [20]. The magnetic structure is shown in Fig. 12.

3.2.4. $TmMn_2Ge_2$

Neutron diffraction patterns recorded at 12 and 1.8 K are presented in Fig. 13. The high temperature pattern, characterized by the magnetic (111), (113) and (201) anti-I lines, displays the classical antiferromagnetic behaviour of the Mn sublattice . The low temperature pattern displays a number of additional peaks. They may be indexed considering a doubling of the c axis. The magnetic order of the thulium moments is therefore similar to the rare earth ordering observed in the RFe_2Si_2 and RFe_2Ge_2 compounds (for a review see Ref. [21]). If we merely consider the contribution of the thulium sublattice, the refinements lead to rather poor agreement factors. However, slight canting of the Mn moment significantly improves the reliability between observed and calculated intensities (Table 4).

The thermal variation of the 001/2 line intensity yields a Néel point of $T_{N2} = 8.5 \pm 0.2$ K (Fig. 5). The magnetic structure is illustrated in Fig. 14(a). The Tm moments are in the (001) planes whilst the Mn moments slightly deviate from the c axis. The Tm ordering gives rise to the sequence + + − −. The component of the Mn moment lying in the (001) plane exhibits the same sequence + + − −. The in-plane component of the Mn atoms located in the ferromagnetic double Tm layers is antiferromagnetically coupled with the surrounding Tm moments.

We note that there is another magnetic arrangement for which only the Mn moments located in the ferromagnetic double Tm layers deviate from the c axis (Fig. 14(b)). Although this arrangement leads to the same calculated magnetic intensities, it has been rejected since it should give rise to spontaneous magnetization ($M \approx 0.3$ μ_B) which is not detected by magnetization measurements.

3.2.5. $LuMn_2Ge_2$

Neutron diffraction patterns recorded between 300 and 2 K are similar to those observed in the case of YMn_2Ge_2 and are consistent with an antiferromagnetic coupling of purely ferromagnetic planes. The refinement of the parameters with data recorded at 2 K

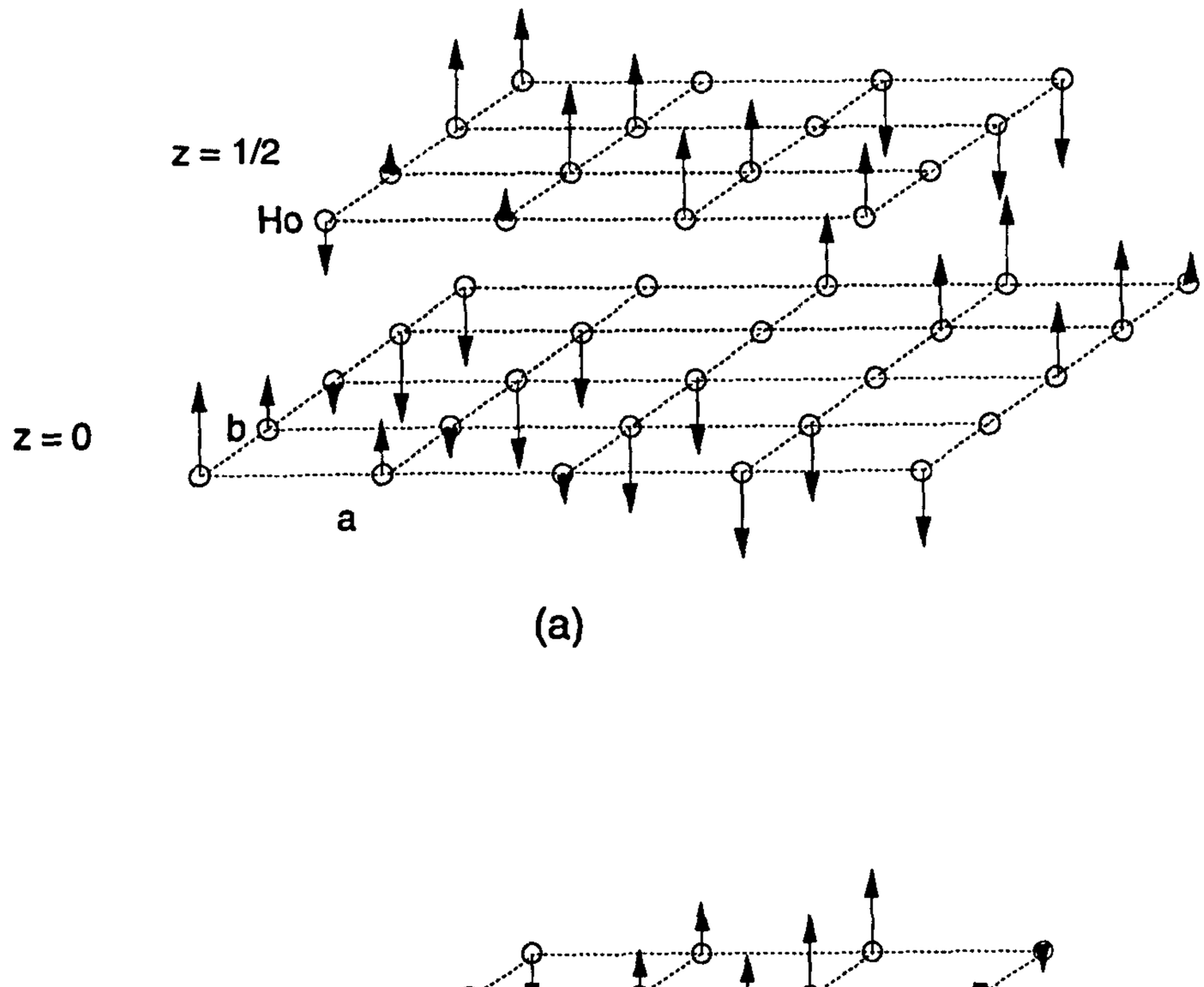

Fig. 10. $HoMn_2Ge_2$: representation of the holmium magnetic sublattice ordering related to each wavevector (a) $q_1 = (0.1543, 0.1543, 0)$; (b) $q_2 = (0.210, 0.007, 0)$.

leads to a manganese moment value of $\mu_{Mn} = 2.32(14)$ μ_B and $z_{Ge} = 0.386(1)$.

4. Discussion

The present study confirms the results of Purwanto et al. [7] and Leciejewicz et al. [6] concerning the magnetic properties of $TbMn_2Ge_2$ and $ErMn_2Ge_2$ respectively. According to this study, the magnetic behaviour of $HoMn_2Ge_2$ has to be revised whilst taking corresponding previous work into account [11]. The magnetic properties of $LuMn_2Ge_2$ are similar to that of YMn_2Ge_2. The magnetic structure of $TmMn_2Ge_2$ is, however, of a new type.

These results enable us to examine and compare the magnetic properties of the whole heavy rare earth compounds. Crystallographic and magnetic properties of the series are summarized in Table 5.

4.1. Magnetic behaviour of the manganese sublattice

Fig. 15 displays the variation of T_N as a function of the cell parameter a for the paramagnetic heavy rare earth compounds and for the solid solution $Y_{1-x}Lu_xMn_2Ge_2$ [15], hence revealing the almost linear relation between T_N and a for the whole series, except for $GdMn_2Ge_2$.

As regards the molecular field approximation, it has been shown, during the study of diamagnetic rare earth compounds $Y_{1-x}Lu_xMn_2Ge_2$ [15], that the variation of T_N and θ_p with cell parameters indicates a

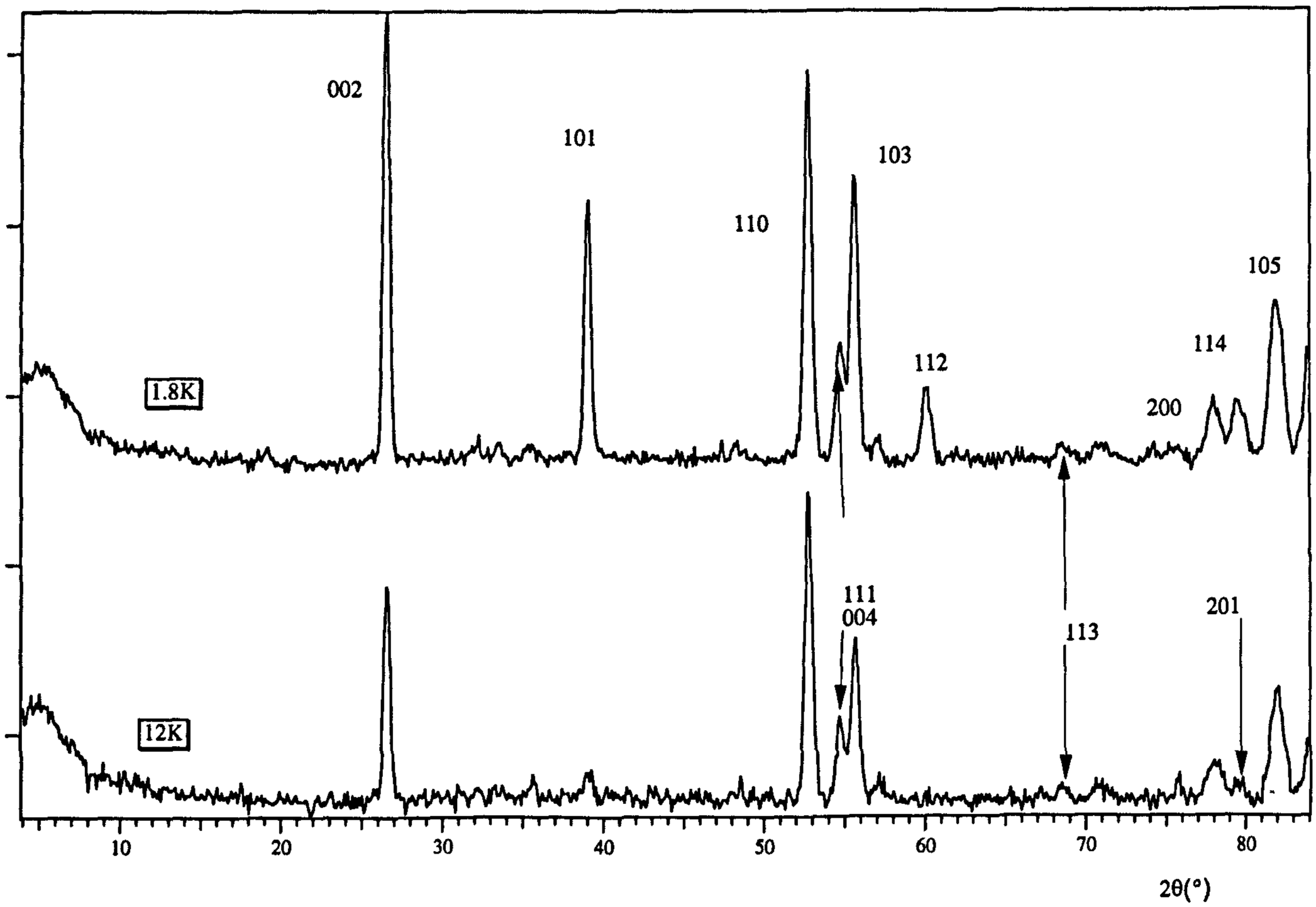

Fig. 11. $ErMn_2Ge_2$: neutron diffraction patterns at 12 and 1.8 K.

Table 3
Observed and calculated structure factors for $ErMn_2Ge_2$ at 12 and 2 K and corresponding refined parameters

	12 K		2 K	
h k l	F_c^2	F_o^2	F_c^2	F_o^2
0 0 2	36.6	37.8(9)	69.8	69.6(5)
1 0 1	8.6	9.7(2)	77.9	80(2)
1 1 0	197.4	195(3)	232.1	229(3)
1 1 1				
0 0 4	59.8	57(3)	86.4	86(2)
1 0 3	117.9	118(3)	191.1	191(3)
1 1 2	3.1	0	67.5	60(3)
1 1 3	14.4	16(3)	16.2	13(3)
2 0 0	54.5	78(5)	78.3	98(5)
2 0 1				
1 1 4	16.2	28(5)	85.9	94(5)
1 0 5	229.4	221(6)	302.6	312(6)
A(Å)	3.953(2)		3.952(2)	
c(Å)	10.802(6)		10.804(6)	
r_c	0.96(1)		0.99(1)	
z_{Ge}	0.387(1)		0.389(2)	
$\mu_{Mn}(\mu_B)$	2.21(22)		2.34(18)	
$\mu_{Ee}(\mu_B)$	0		6.81(31)	
R(%)	8.4		6.2	

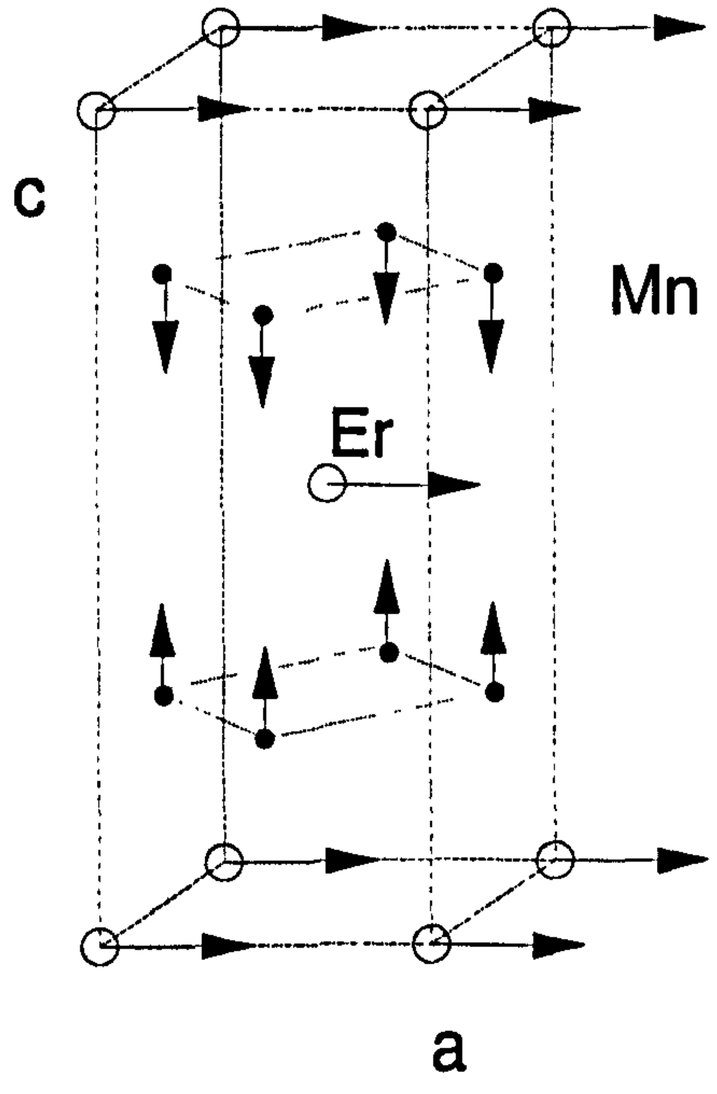

Fig. 12. Magnetic structure of $ErMn_2Ge_2$ at 1.8 K.

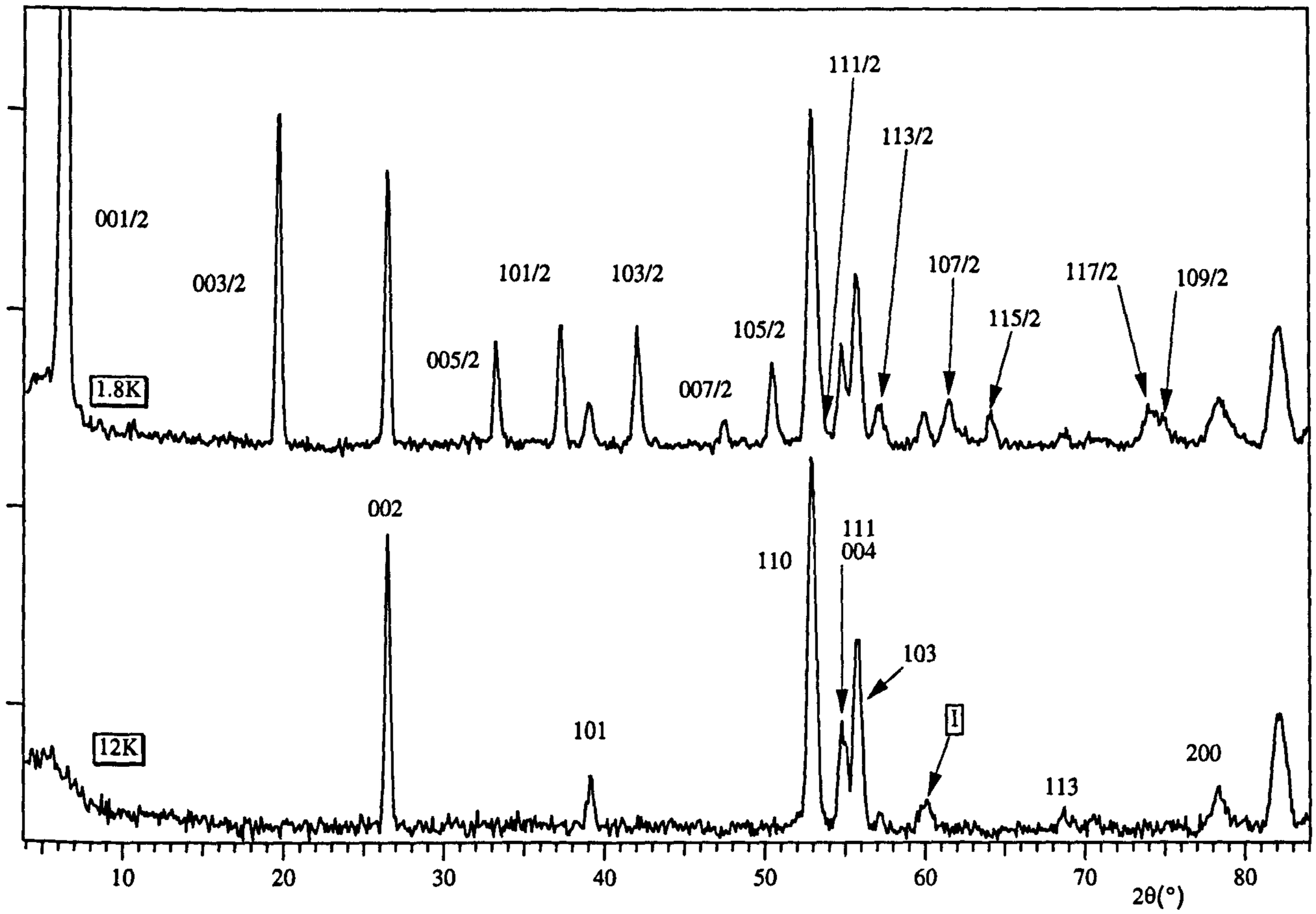

Fig. 13. $TmMn_2Ge_2$: neutron diffraction patterns at 12 and 1.8 K.

strengthening of the antiferromagnetic interplane interactions when a decreases.

Since the Néel temperature of the paramagnetic rare earth compounds fits the general variation measured in diamagnetic rare earth compounds fairly well, it is suggested that the RMn_2Ge_2 (R = Gd, Tb, Dy, Er, Tm) series will follow the same trend.

The variation of the Mn moment value with a (Fig. 16) indicates that the magnitude of the moment is almost constant and about 2.3 μ_B for the heavy rare earth compounds whereas it increases continuously in the light rare earth series. This observation suggests that the Mn atoms are not in the same electronic state in the heavy and light rare earth compounds. The variation of the interatomic distances along the whole series is probably responsible for this phenomenon.

4.2. Rare earth magnetic ordering

The magnetic properties of the rare earth sublattices exhibit a greater variety of behaviour, probably sustained by various phenomena such as the relative strength of the Mn–Mn, R–Mn and R–R interactions and the magnetocrystalline anisotropy.

As regards the previous section, it is suggested that the larger are the cell parameters, the weaker is the Mn–Mn antiferromagnetic interplane coupling. In contrast, according to a study conducted by Brooks et al. [22] and reported in Ref. [23], the R–T interaction is expected to vary with the quantity

$$J_{4f,5d} \propto 94 - 3.4(x - 1)$$

where $x = 1$ for Gd, 2 for Tb, etc., such that, within the heavy rare earth compounds, the strongest R–T interaction is expected in the Gd compound and decreases by about 3% in each of the subsequent rare earth compounds.

Therefore, it is apparently easier to align the Mn sublattice under the effect of the internal field induced by the R–Mn interactions in the largest rare earth compounds, since, in this case, J_{Mn-Mn}(interplane) is weaker while J_{R-Mn} is greater. This trend seems to be fairly respected for the first examples of the series,

Table 4
Observed and calculated intensities and corresponding refined parameters for $TmMn_2Ge_2$ at 12 and 2 K

	12 K		2 K		
h k l	F_c^2	F_o^2	F_c^2 (Tm)	F_c^2 (Tm + Mn)	F_o^2
0 0 1/2			11.6	10.9	10.78(7)
0 0 3/2			10.9	20.1	19.5(3)
0 0 2	28.1	28.7(6)	26.8	27.9	28.2(5)
0 0 5/2			9.2	17.1	16.1(5)
1 0 1/2			22.6	26.3	26.2(8)
1 0 1	10.7	12(1)	13.1	11.8	13(1)
1 0 3/2			23.7	28.5	33(1)
0 0 7/2			7.2	6.7	8.0(9)
1 0 5/2			22.4	27.9	35(1)
1 1 0	187.7	187(3)			
1 1 1/2			236.2	225.4	210(3)
1 1 1					
0 0 4	53.2	55(3)	53.4	54.4	54(2)
1 0 3	106.8	107(3)	96.9	100.9	106(2)
1 1 3/2			16.2	13.2	26(2)
1 0 7/2			18.6	23.9	37(4)
0 0 9/2			5.2	4.8	11(5)
1 1 5/2			15.3	12.8	22(2)
1 1 3	13.5	13(2)	11.3	13.2	14(2)
1 1 7/2					
1 0 9/2			26.9	40.9	40(4)
2 0 0	49.7	55(5)			
0 0 11/2					
2 0 1/2			71.9	67.6	76(4)
2 0 1					
1 1 4	16.5	11(5)	15.0	16.6	20(4)
2 0 3/2					
1 0 5	186.9	179(5)	194.3	202.2	216(4)
a(Å)	3.934(1)		3.933(2)		
c(Å)	10.781(4)		10.775(6)		
r_c	0.99(1)		1.01(1)	1.00(1)	
z_{Ge}	0.385(1)		0.388(4)	0.386(1)	
$\mu_{Mnz}(\mu_B)$	2.19(11)		1.95(7)	2.28(27)	
$\theta_{canting}(°)$	0		0	21(3)	
$\mu_{Tm}(\mu_B)$	0		5.96(41)	6.63(18)	
R(%)	3.9		16.4	11.0	

yielding a ferrimagnetic ordering with Curie point decreasing from Gd to Dy (Table 5).

Nevertheless, in such a description, it is rather surprising to find the same Curie temperatures for $GdMn_2Ge_2$ and $TbMn_2Ge_2$. This rather peculiar behaviour of $GdMn_2Ge_2$ might arise from its situation at the limit between the RMn_2Ge_2 compounds characterized by ferromagnetic Mn (001) planes and those characterized by mixed Mn (001) planes. In this case, the lowering of the Curie temperature might be caused by modifications of the Mn electronic state that is also suggested by the anomaly concerning the corresponding Néel temperature (Fig. 15).

The $HoMn_2Ge_2$ and $ErMn_2Ge_2$ compounds are characterized by an antiferromagnetic arrangement of the ferromagnetic Mn planes which still remains in the ordered rare earth state. In these compounds, the R–Mn interactions are unable to align the Mn moments and it is assumed that the R–Mn interactions no longer intervene. Therefore, the rare earth ordering should merely arise from the R–R interactions and it is rather surprising that the de Gennes scaling does not account for the rare earth ordering temperature in these compounds (Table 5).

Such behaviour may be due to magnetocrystalline anisotropy effects. The uniaxial anisotropy of holmium tends to align the moments along the *c* axis yielding a highly frustrated situation within which the holmium (001) planes are surrounded by antiferromagnetically coupled ferromagnetic Mn planes. Inversely, the positive Stevens factor value of erbium tends to locate the Er moments in the basal plane where they are magnetically decoupled from the Mn magnetic sublattice which remains antiferromagnetic in the whole temperature range from T_N to 2 K, with the Mn moment aligned along the *c* axis.

Finally, $TmMn_2Ge_2$ is a special case. It is the first RMn_2Ge_2 compound where the + + − − sequence is observed. Moreover, it is characterized by a canting of the Mn moments which is neither observed in $HoMn_2Ge_2$ nor in $ErMn_2Ge_2$ where the R–Mn interactions are expected to be greater, according to the calculations of Brooks et al. [22].

As the assumptions of an enhancement of the R–Mn interactions or a weakening of the nearest neighbour Mn–Mn interplane interactions may be ruled out, one has to assume that the + + − − sequence is

Table 5
Summary of the cell parameters (measured at 300 K with Si as internal standard) and magnetic properties of the compounds RMn_2Ge_2 (R = yttrium and heavy rare earths)

	Y	Gd	Tb	Dy	Ho	Er	Tm	Lu
a(Å)	3.9945(6)[a]	4.0261(6)[a]	4.0080(7)[a]	3.9921(7)[a]	3.9765(9)[a]	3.9647(5)[a]	3.9541(7)[a]	3.9388(5) [15]
c(Å)	10.865(2)[a]	10.877(2)[a]	10.868(3)[a]	10.858(3)[a]	10.848(3)[a]	10.837(2)[a]	10.823(3)[a]	10.809(2) [15]
T_N(Mn)(K)	427 [15]	365 [10]	414 [10]	438 [10]	459 [10]	475 [10]	487[a]	508 [15]
T_t(R)(K)	–	96 [10]	95 [10]	40 [10]	2.1[a]	5.5[a]	8.5[a]	–
$\mu_{Mn}(\mu_B)$	2.23 [3]	–	2.21[a]	2.3 [4]	2.38[a]	2.34[a]	2.28[a]	2.32[a]
$\mu_R(\mu_B)$	–	–	8.81[a]	10.2 [4]	6.9[a]	6.81[a]	6.63[a]	–

[a] Present study.

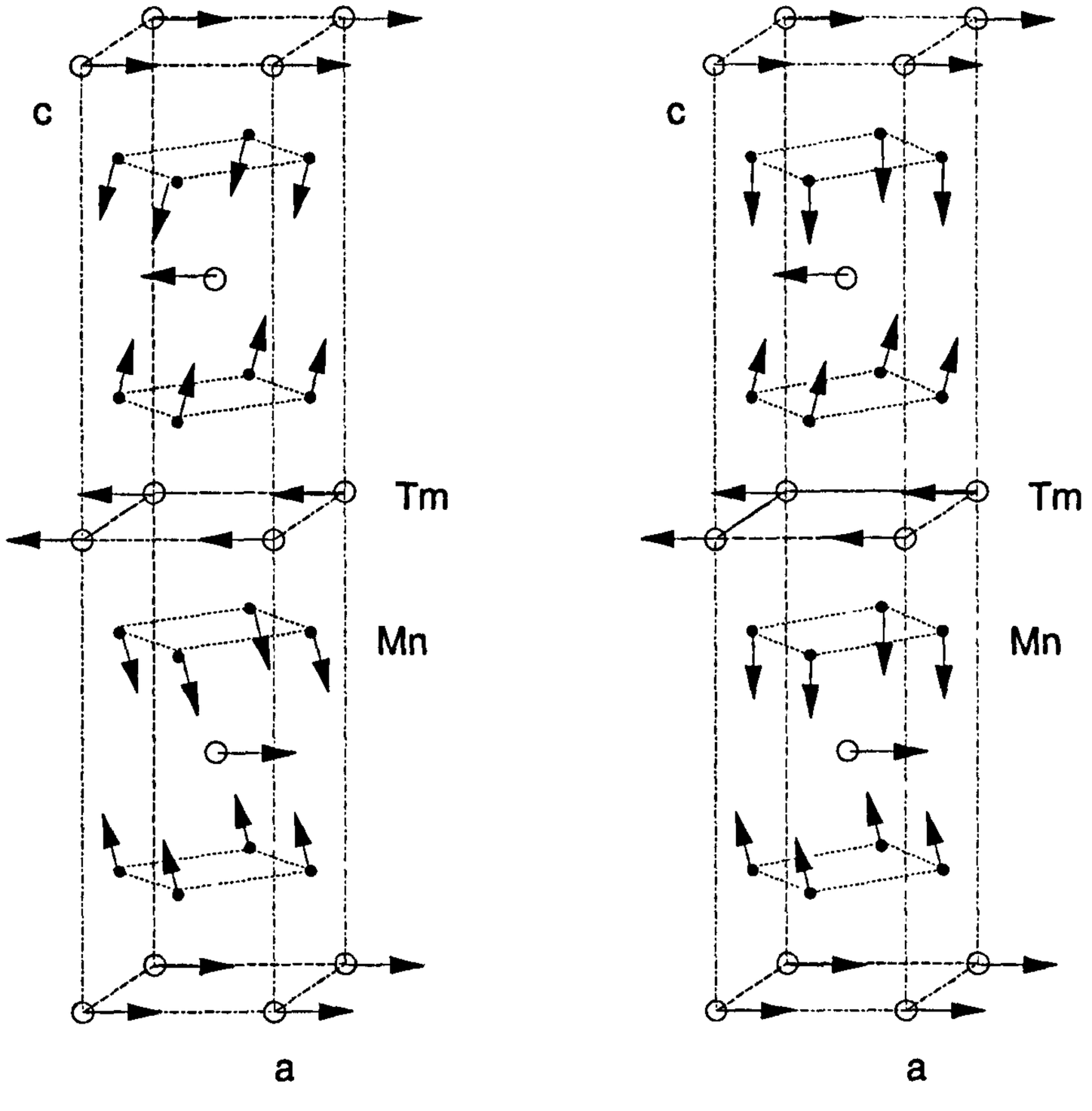

(a) (b)

Fig. 14. Magnetic structure of $TmMn_2Ge_2$ at 1.8 K.

particularly favourable for the Mn magnetic sublattice i.e. that the next-nearest neighbour Mn–Mn interactions might be antiferromagnetic. Such an assumption could be related to the magnetic behaviour of $DyMn_2Ge_2$ and $TbMn_2Si_2$ [5,7] characterized by magnetic superstructures where both ferro- and antiferromagnetic next-nearest neighbour interplane couplings coexist.

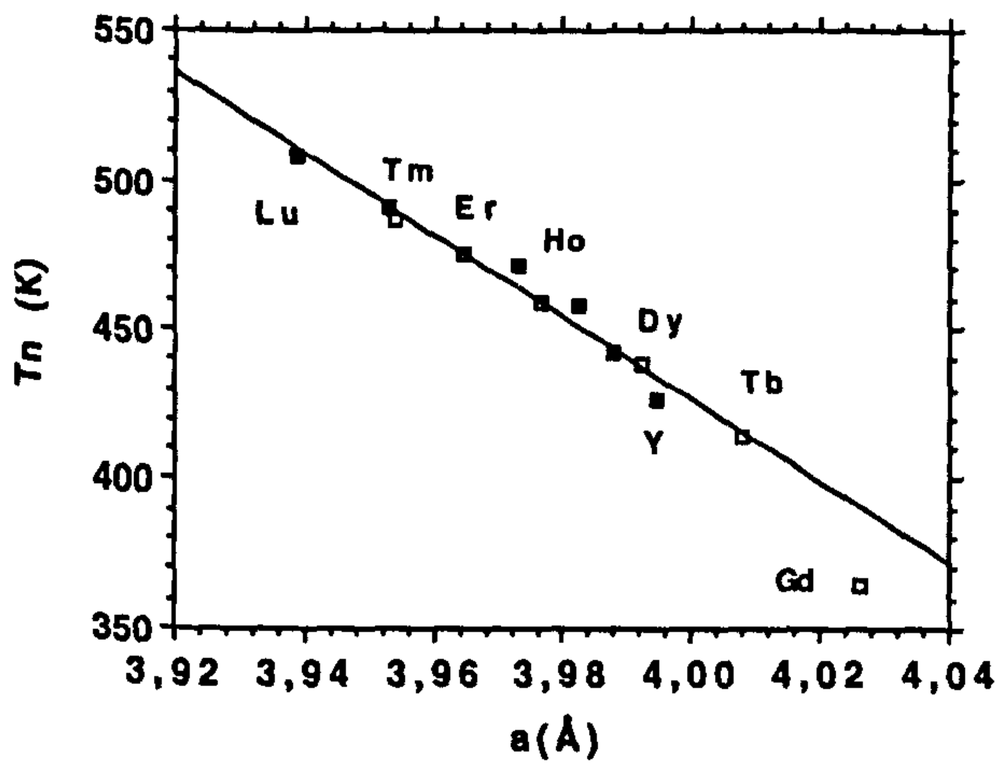

Fig. 15. Variation of the Néel temperature vs. the cell parameter *a* for the RMn_2Ge_2 heavy rare earth compounds (empty symbols) and for the solid solution $Y_{1-x}Lu_xMn_2Ge_2$ (full symbols).

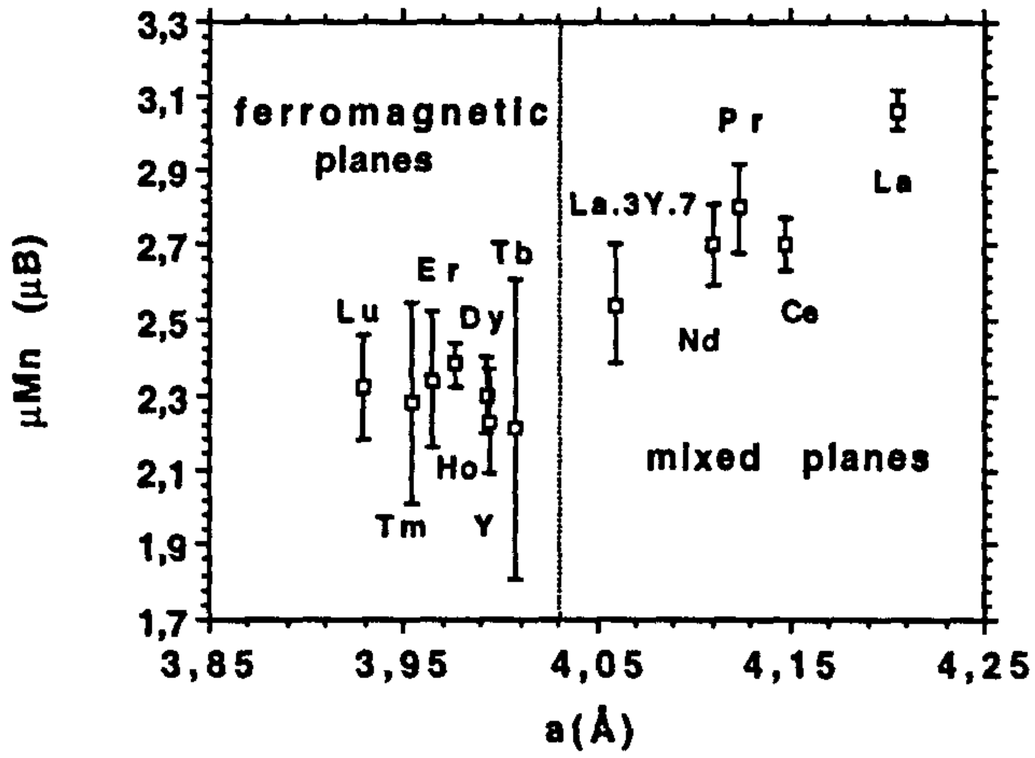

Fig. 16. Variation of the Mn moments vs. the cell parameter *a* for the whole RMn_2Ge_2 series (R = Y, La–Nd, Tb–Tm, Lu).

5. Conclusions

This neutron diffraction study provides interesting information. Within the newly studied compounds, the magnetic properties of the Mn sublattice are in good accord with previous results. The rare earth magnetic sublattice displays a great variety of magnetic behaviour which is mainly a consequence of the evolution of the relative strengths of the Mn–Mn and R–Mn interactions. The observed discrepancies from this general scheme might arise from additional underlying phenomena which are still not fully understood. Further investigations, particularly involving solid solutions within which the R–Mn and Mn–Mn interactions are made to vary, should provide further information.

References

[1] G. Venturini, R. Welter, E. Ressouche and B. Malaman, *J. Alloys Comp., 210* (1994) 213.
[2] R. Welter, G. Venturini, E. Ressouche and B. Malaman, *J. Alloys Comp., 218* (1995) 204.
[3] G. Venturini, R. Welter, E. Ressouche and B. Malaman, *J. Alloys Comp., 223* (1995) 101.
[4] H. Kobayashi, H. Onodera, Y. Yamaguchi and H. Yamamoto, *Phys. Rev. B, 43* (1) (1991) 728.
[5] G. Venturini, B. Malaman, K. Tomala, A. Szytula and J.P. Sanchez, *Phys Rev. B, 46* (1) (1992) 207.
[6] J. Leciejewicz, S. Siek and A. Szytula *J. Magn. Magn. Mater., 40* (1984) 265.
[7] S. Purwanto, M. Ohashi, H. Onodera, Y. Morii, S. Funahashi, H. Yamauchi and Y. Yamaguchi, *Proc. Fifth Int. Symp. on Advanced Nuclear Energy Research, 1993*, Vol. 2, p. 447.
[8] J. Leciejewicz and A. Szytula, *Solid State Commun., 49* (4) (1984) 361.
[9] A. Gil, J. Leciejewicz, K. Maletka, Z. Tomkowicz and K. Wojciechowski, *J. Magn. Magn. Mater., 129* (1994) L155.
[10] T. Shigeoka, *J. Sci. Hiroshima Univ. Ser. A, 48* (2) (1984) 103.
[11] J. Leciejewicz, A. Szytula, W. Bazela and S. Siek, *J. Magn. Magn. Mater., 89* (1990) 29.
[12] C. Stassis, H.W. Deckman, B.N. Harnan, J.P. Desclaux and A.J. Freeman, *Phys. Rev. B, 15* (1977) 369.
[13] C.G. Shull and Y. Yamada, *J. Phys. Soc. Jpn., 22* (1962) 1210.
[14] P. Wolfers, *J. Appl. Crystallogr., 23* (1990) 554.
[15] G. Venturini, *J. Alloys Comp., 232* (1996) 133.
[16] M. Duraj, R. Duraj, A. Szytula and Z. Tomkowicz, *J. Magn. Magn. Mater., 73* (1988) 240.
[17] E.M. Gyorgy, B. Batlogg, J.P. Remeika, R.B. van Dover, R.M. Fleming, H.E. Blair, G.P. Espinosa, A.S. Cooper and R.G. Maines, *J. Appl. Phys., 61* (1987) 4237.
[18] K. Tomala, J.P. Sanchez, B. Malaman, G. Venturini, A. Blaise, R. Kmiec and E. Ressouche, *J. Magn. Magn. Mater., 131* (1994) 345.
[19] M. Ohashi, K. Koizuka, H. Onodera, H. Yamauchi, Y. Yamaguchi, T. Kaneko and S. Funahashi, *Physica B, 213–214* (1995) 312.
[20] A. Szytula, M. Slaski, J. Kurzyk, B. Dunlap, Z. Sungaila and A. Umezawa, *J. Phys., 48* (C8) (1988) 437.
[21] A. Szytula and J. Leciejewicz, Magnetic properties of ternary intermetallic compounds of the RT_2X_2 type, in K.A. Gschneidner, Jr. and L. Eyring (eds.), *Handbook on the Physics and Chemistry of Rare Earths*, Vol. 12, Elsevier, Amsterdam, 1989, Chapter 83, p. 133.
[22] M.S.S. Brooks, L. Nordström and B. Johansson, *Physica B, 173*, (1991) 95.
[23] K.H.J. Buschow, *Rep. Prog. Phys., 54* (1991) 1123.